



# Along-strike pre-orogenic thickness variation and onlapping geometries control on thrust wedge evolution: insights from sandbox analogue modelling

S. BIGI<sup>1\*</sup>, C. GALUPPO<sup>2</sup>, L. PERFETTI<sup>3</sup>, S. COLELLA<sup>4</sup> AND M. CIVALLERI<sup>4</sup>

<sup>1</sup>*Dipartimento di Scienze della Terra, Università degli Studi di Roma "La Sapienza", P.le Aldo Moro 5 - 00183, Roma, Italy.*

<sup>2</sup>*Via della L. Lombarda, 22, Roma, Italy.*

<sup>3</sup>*Via I. Ciampi, 18, Roma, Italy.*

<sup>4</sup>*Via Monza, 30, Roma, Italy.*

*\*e-mail: sabina.bigi@uniroma1.it*

---

**Abstract:** Thickness variation of sedimentary sequences is largely viewed as a controlling factor on the evolution of orogenic wedges; among the different structural and stratigraphic features generating thickness variation, we focused our analysis on the onlapping geometries, using laboratory sandbox experiments. The aim was trying to describe how a common sedimentary configuration could influence thrusts geometry and mode of accretion. Model results showed that onlapping geometries in pre-tectonic sediments cause a great complexity, dominated by curvilinear thrusts, back thrust and out-of-sequence thrusts. They also influence mode of accretion, generating diachronous thrusting along strike, reactivation and under-thrusting alternating to simple piggy-back sequence. Our modeling results are compared with natural examples from the Apennines, the southern Pyrenees, the Pindos (Greece) and the West Spitsbergen (Greenland) fold and thrust belts, among many others, where strain localization and diachronic thrusting affecting thrust propagation in correspondence to complex geometries both in the pre-orogenic stratigraphy and in the upper crust.

**Keywords:** analogue models, orogenic wedge, thickness variation, onlap, thrust sequence.

---

Thickness variation in pre-orogenic sedimentary successions is a common feature in convergent margins. It can be due to depositional features (Speed *et al.*, 1984), to differential compaction depending on different palaeogeographic settings (Carminati and Santantonio, 2005), to the occurrence of basement highs in the foreland (Thomas, 1990; Doglioni *et al.*, 1994) and to structural control, as for example, the activity of normal faults during the evolution of the previous passive margin stage (Gilchrist *et al.*, 1987;

Butler, 1989). Among all of them, we performed sandbox analogue models to investigate the influence of along-strike onlapping geometries on the three-dimensional architecture of a fold-and-thrust-belt.

Analogue modelling is a valuable tool for studying the evolution of orogenic wedge accreting from constant thickness sand pack both in two and in three dimensions (Malavieille, 1984; McClay, 1990; Storti *et al.*, 2000). Sand box models using

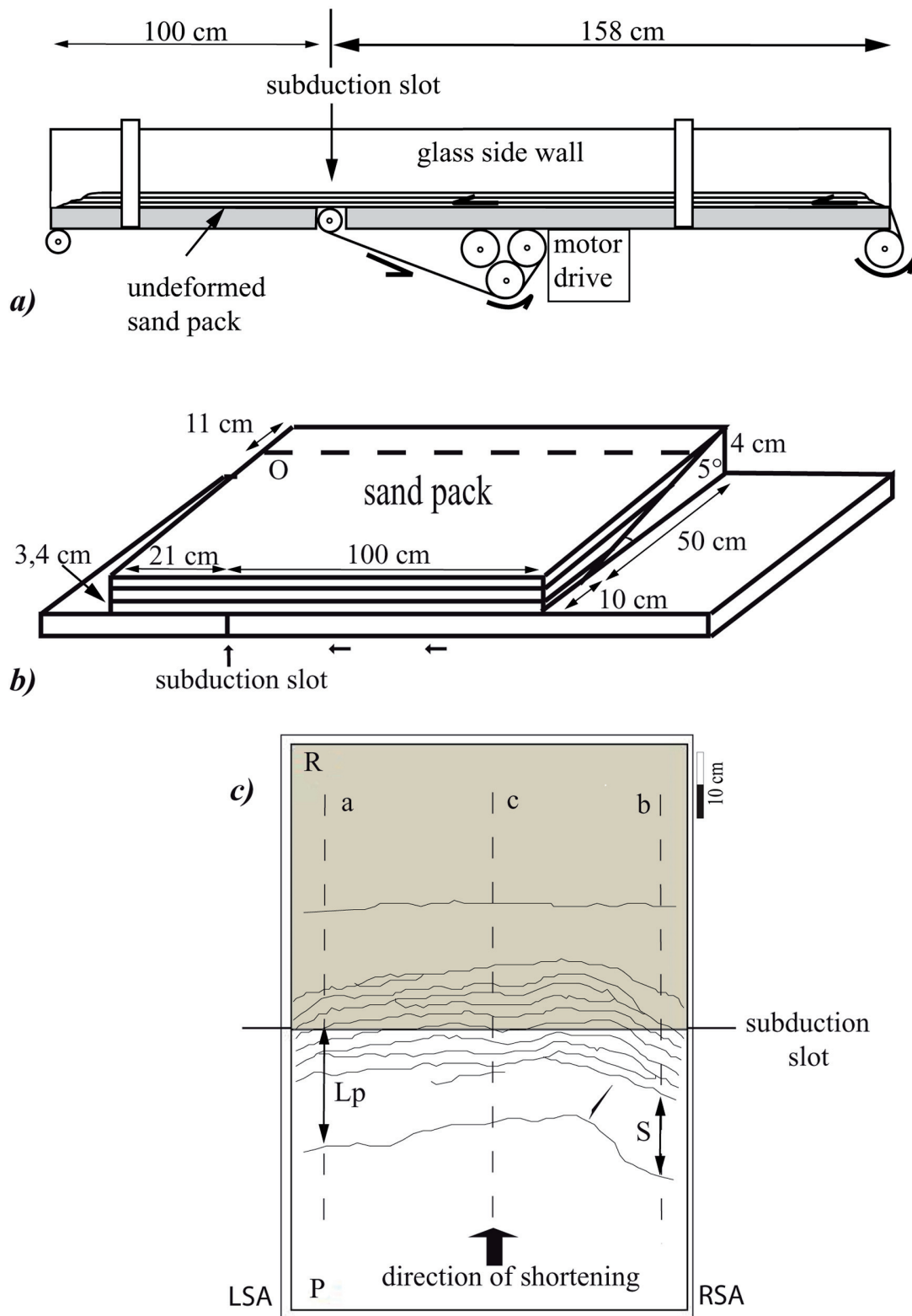


**Figure 1.** (a) Experimental apparatus used for double-verging sand wedge models, (b) simplified sketch illustrating the basic configuration of the models (in gray, the depositional slope), (c) map view of the model showing the measured parameters along sections a, b, c;  $L_p$  and  $S$ . Lines O and D indicate the end of the onlap onto the depositional slope and the end of the depositional slope onto the film draft, respectively.

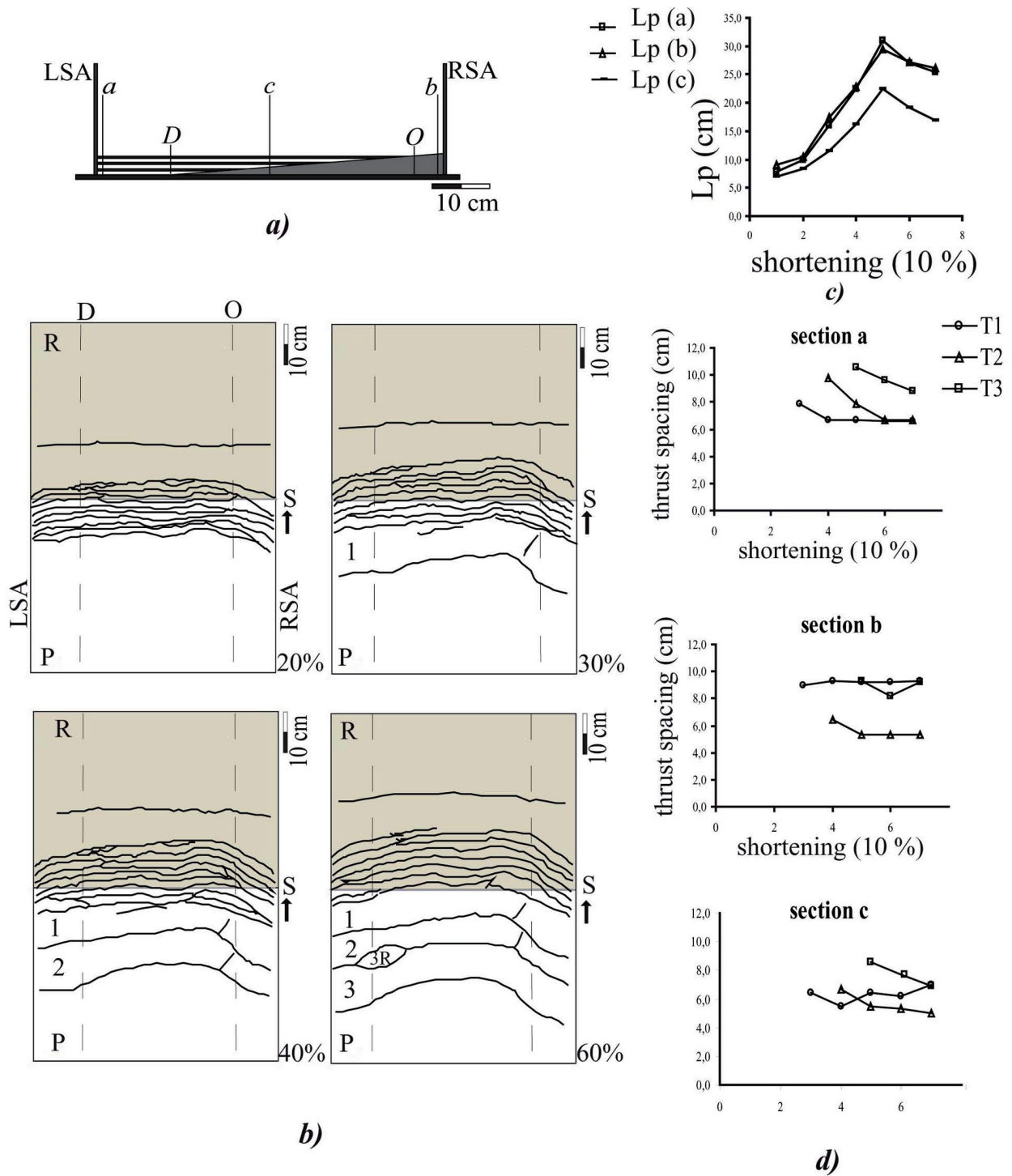


**Figure 2.** (a) Initial geometry of model E1 with sections a, b, c, O (end of the onlapping sequence) and D (end of the depositional slope) (view in the direction of shortening), (b) line drawings (from map view photographs) of sequential evolutionary stages every 10% of shortening, (c) prowedge length (Lp) vs. shortening diagram, illustrating the progressive evolution of the deformation fronts. The length is measured along the three sections a, b and c located in figure 2a. Note as the central zone of the model always retreated with respect to the other two and that nucleation of thrust happened alternatively on the left and on the right side, (d) thrust spacing vs. shortening along cross sections a, b and c. Note as in the central zone (section c) all the thrust planes are active together.

simple along-strike tapering geometries have already highlighted that thrust wedges accreting from pre-orogenic tapering sedimentary series evolve in a non-cylindrical fashion, and that thickness variation plays a first order role in determining the three-dimensional architecture of the resulting orogenic belt (Mulugeta, 1988; Marshak and Wilkerson, 1992; Boyer, 1995; Storti *et al.*, 2001; Soto *et al.*, 2003).

In our models, we add to the simple tapering geometry an onlapping sedimentary sequence that reduces its thickness in the opposite direction with respect to the depositional slope, striking parallel to the direction of subduction (Fig. 1). This configuration simulates the along strike thickness variation commonly described, for example, in the foredeep systems, where turbiditic siliciclastic sequences progressively onlap along the main axes of the basin. In the Apennines foredeep system, for example, the Lower Pliocene sequence varies its thickness from north to south several times along the main direction of the basin (Ori *et al.*, 1991; Bigi *et al.*, 1992; Bigi *et al.*, 1997 and references therein).

## Methods and materials

The used apparatus is a 2.58 m long deformation rig with two glass walls of the same length separated by a 60 cm width (Fig. 1). All experiments were performed under normal gravity conditions. Dry, non-cohesive quartz sand with 190  $\mu\text{m}$  grain size (coefficient of friction  $\mu=0.55$ ) (McClay, 1990; Liu *et al.*, 1992) and an average density of  $1.58\pm 0.1\text{ g cm}^{-3}$  was used to simulate brittle deformation (Storti, 1997). Aluminium microspheres were used to simulate a mechanical behaviour of weaker layers within the sedimentary successions in experiment E2 and E3 (Rossi and Storti, 2003). The drafting film used to simulate the basal detachment was characterized by a high coefficient of friction ( $\mu_b=0.55$ ) equal to the coefficient of friction of quartz sand. Using a scaling factor of  $10^{-5}$ , 1 cm in the models represents  $\sim 1$  km in upper-crustal rocks (Liu *et al.*, 1992).

We designed the configuration of pre-contractual sediment package in order to simulate a depositional slope covered by an onlapping sedimentary sequence. The slope was oriented parallel to the direction of subduction and dips  $5^\circ$ ; its thickness varies from 4 cm on the right side of the apparatus (RSA) to zero at about 10 cm from the other side (Fig. 1). The sedimentary sequence onlaps onto the slope and covers it quite completely, as illustrated in figure 1b, where the

line O indicates the end of the onlap onto the depositional slope; its thickness varies from 3.4 cm from the left side (LSA) to zero on the slope. We used only dry sand in E1 experiment and reconstructed the same geometry in the other two experiments introducing a weaker layer onto the slope in the E2 model, and inside the onlapping succession in E3 experiment. The configuration of each experiment is illustrated in figures 2, 3 and 4.

Deformation was induced by pulling the basal detachment sheet by a motor drive ( $6.67\text{ cm h}^{-1}$ ) down into a thin subduction slot located 100 cm from the front end of the sand layers apparatus (Figs. 1a and 1b). The bottom of the deformation rig, from the subduction slot to the back end of the apparatus (at a distance of 21 cm) was floored with the same drafting film in order to ensure the same basal frictional characteristics over the whole model. According to Storti *et al.* (2000), we define the prowedge as the region in front of the subduction slot, where material moves toward it and the dominant transport direction is opposite to the motion of the detachment sheet. The retrowedge is the region behind the subduction slot, where there is no relative motion between the rigid base plate and the overlying material, and the drifting film is fixed. The axial zone is the flat region between the previous two.

In order to describe the growing thrust wedge we use the following parameters: i)  $L_p$  is the distance of the deformation front from the subduction slot in the prowedge, and ii)  $S_n$  is the distance between a deformation front (n) and the previous one. These two values were plotted against shortening ratio, expressed in terms of  $Sh=L_1/L_0\times 100$ , where  $L_0$  is the initial sand pack length and  $L_1$  is the progressive shortening applied to the sand pack. We measured these distances every 10% of shortening from map views along three sections: a) and b), each of them at 5 cm from the two glasses (and at a distance of 50 cm each other), and c) at the centre on the model (Fig. 1c).

## Results

The used experimental apparatus, generates a double-verging accretionary wedge showing two stages of evolution, according to all the other models well documented in literature both for constant and tapering sand packs (Malavieille, 1984; Liu *et al.*, 1992; Storti *et al.*, 2000, among many others). Therefore, the first part of all the experiments was characterised by rapid uplift of the axial zone and by rapid back thrusting along a retro-verging thrust ramp together with the development of closely spaced pro-verging kink bands

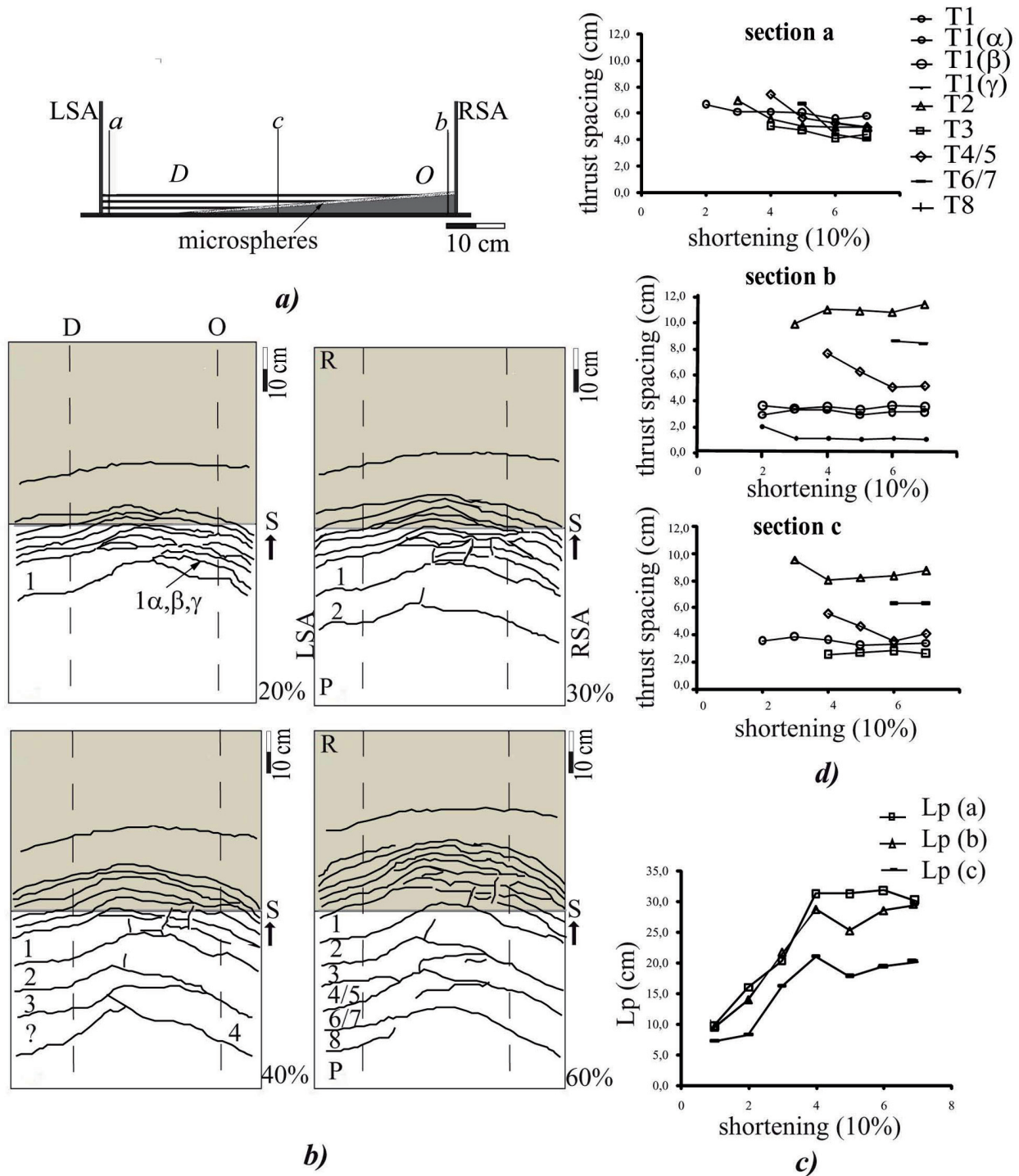


**Figure 3.** (a) Initial geometry of model E2 with sections a, b, c, O (end of the onlapping sequence) and D (end of the depositional slope), (b) line drawings (from map view photographs) of sequential evolutionary stages every 10% of shortening, (c) prowedge length (Lp) vs. shortening, illustrating the progressive evolution of the prowedge deformation fronts. The length is measured along the three sections a, b and c located in figure 3a. Note as the central zone Lp (c) always retreated with respect to the other two and that nucleation of thrust happened alternatively from the left and from the right side, (d) thrust spacing vs. shortening along cross sections a, b and c. Note as in the central part most of shortening is localized on T4/5 thrust.

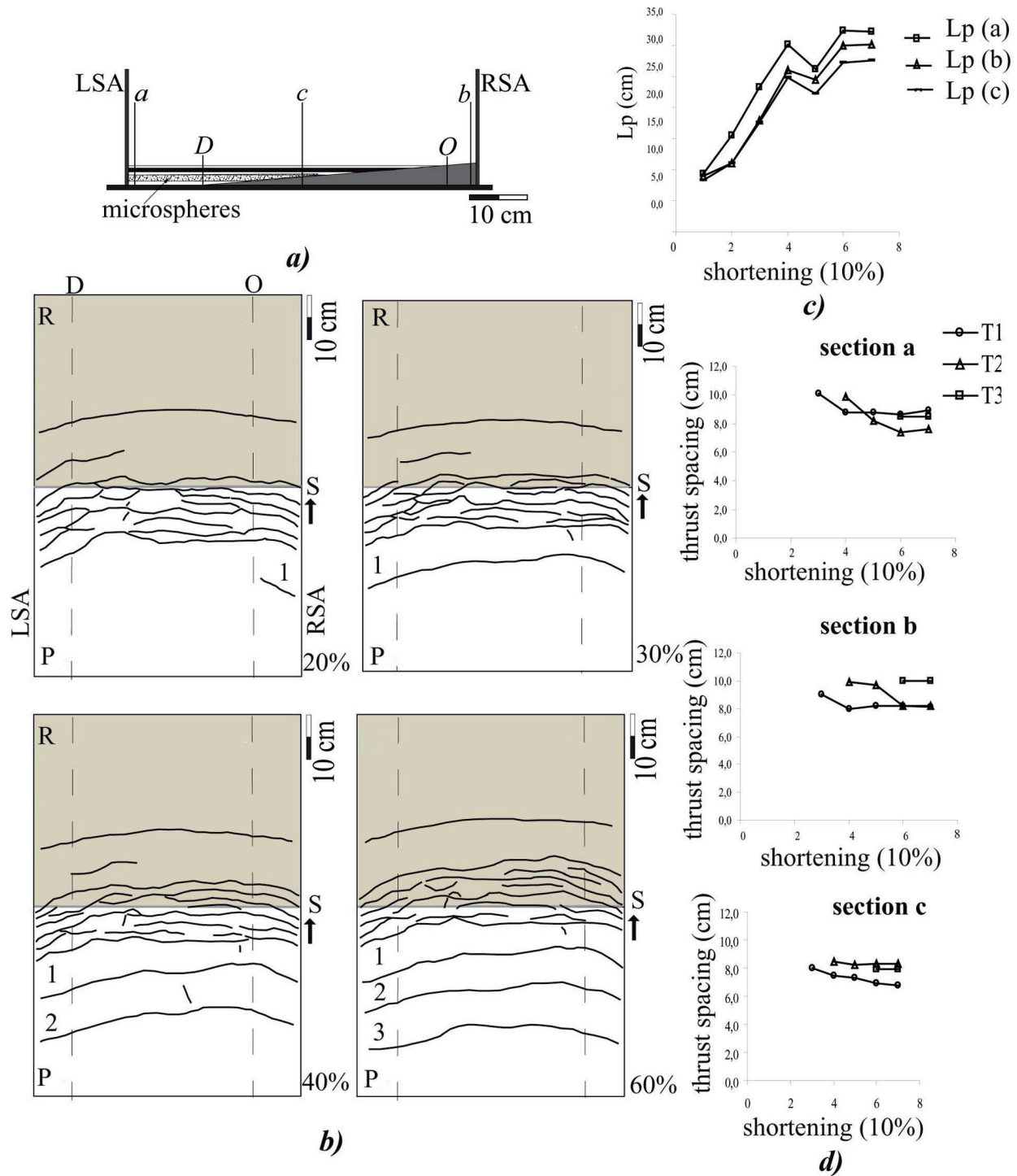


**Figure 4.** (a) Initial geometry of model E3 with sections a, b, c, O (end of the onlapping sequence) and D (end of the depositional slope), (b) line drawings (from map view photographs) of sequential evolutionary stages every 10% of shortening, (c) prowedge length (Lp) vs. shortening diagram, illustrating the progressive evolution of the deformation fronts. The length is measured along the three sections a, b and c located in figure 4a, (d) thrust spacing vs. shortening along cross sections a, b and c.

at the subduction slot. The second stage of evolution, consisting of the accretion of the prowedge, is characterised by the nucleation of a thrust front far from the subduction slot at 21% of shortening in E1 experiment, at 15% in E2 and at 21% in E3 model. Moreover, during the first stage of evolution, the high frequency of kink bands shows variation along strike; in all the experiments we observed the occurrence of lateral ramps and anastomosing structures developed in correspondence of the end both of the onlapping sequence and of the depositional slope (along sections O and D; figures 2, 3 and 4).

#### *Basic model E1*

In E1 model we used only dry sand to build up the experiment; differences in the sand could be due to different compaction obtained by different ways to set the sand itself (bed by bed in the onlapping sequence and all at the same time in the depositional slope) (Fig. 2a). After 22% of shortening the first thrust, T1, was nucleated far from the subduction slot and progressively incorporated into the axial zone, which increased its height. T1 started in the sedimentary succession on the left side of the apparatus (LSA) and propagated laterally towards the right side (RSA) that reached at 24% of shortening. The T1 geometry shows a curvature along strike with the more advanced zone developed along the right and the left sides. The second thrust, T2, nucleated at 33% at the LSA, propagated laterally at 34% to RSA, whereas the third thrust front T3 started contemporaneously at 48%. The experiment ended at 68% of shortening. The variation of  $L_p$  during the deformation and also the final geometry, clearly illustrates the influence of the two tapering structures, showing a central zone, corresponding to the tapering of the slope and of the onlapping multilayer (lines D and O), systematically retreated with respect to the lateral sides, where both of them have the maximum thickness (Fig. 2c). Nucleation of thrusts T1 and T2 is diachronic of about 2% of shortening; thrusting started on the LSA of the model and reached the other side propagating laterally. The distribution of displacement on each thrust shows a different organization along the three sections during thrusting (Fig. 2b). On the left and right sides (section a and b), a piggy-back sequence can be observed, with a reduced component of synchronous thrusting; along section c, instead, synchronous thrusting follows an “in sequence” generation of the thrust fronts, to balance the retreating position of thrust fronts (Fig. 2d).

#### *Model E2*

In E2 model, a weaker layer, made of aluminium microsphere, 2 mm thick, was located on the depositional slope under the multilayer onlapping succession; the obtained configuration is illustrated in figure 3a. After 15% of shortening, the prowedge started to propagate and the first thrust front nucleated on LSA. T1 propagated laterally until the central part of the apparatus. Immediately after, between 15% and 20%, three thrust fronts, closely spatiated, started on RSA, in the footwall of T1 (T1  $\alpha$ ,  $\beta$ ,  $\gamma$ , figure 3b). Deformation proceeded with the nucleation of T2 thrust at 24%, showing a linear geometry in map view. This can be due to a smaller shortening accommodated by the previous thrusts in the central part of the model. The next three thrust fronts propagated from one side of the apparatus to the centre of the model, without reaching the other side. The T3 thrust started from LSA at 35%, the T4 started from RSA at 39% and T5 from LSA at 40%. From 40% to 50% of shortening, in the transfer zone between T4 and T5 thrust fronts, tear faults developed, becoming a single, rectilinear thrust front. Until 59%, other three thrust fronts generated as the previous ones, T6 and T7, respectively at 50% and at 52% of shortening evolved in one thrust front at 55% of shortening, while at 59%, T8 propagated from LSA to the centre of the model. The experiments ended at 64% of shortening (Figs. 3c and 3d).

#### *Model E3*

In E3 model, in order to vary the mechanical behaviour of the onlapping succession, the bottom of the multilayer succession consists of a layer of microsphere, 1.2 cm thick, placed onto a 0.7 cm thick layer of white sand (Fig. 4a). After 20% of shortening, the prowedge started to accrete with a thrust front (T1) highly curved, generated on RSA and propagated just until the O line (Fig. 4b). It remained active until 23%, when on the LSA another thrust front propagated laterally until RSA linking to T1; after that moment they remain active as a single thrust front (T1 in figure 4). The anticlines associated with T1 thrust showed a box fold shape and evolved in a back thrust on the back limb during deformation. This back-thrust can be followed laterally in the multilayer onlapping sequence until 20 cm from the RSA. At 35–36%, T2 quickly propagated laterally from LSA; even this thrust front and an associated back-thrust occurred just in the onlapping sequence, until 35 cm from the RSA. At 53%, the last thrust front, T3, generated synchronously; following its structural style laterally, this front shows, as the previous ones, an asso-

ciated back-thrust developed in the multilayer sequence, that occurs until 25 cm from the RSA. The experiments ended at 62% of shortening.

## Discussion

In all our experiments, we simulated thickness variations in three different configurations. In E1 model, we use just dry sand, and mechanical variations were due to differential compaction generated by the onset of the model itself. In E2 model, a weaker layer, located on the top of the depositional slope, decouples the two tapering structures. In E3 model, we differentiated the mechanical behaviour of the onlapping sequence constructing a more efficient layer close to its bottom (Figs. 2a, 2b, 3a, 3b, 4a and 4b).

In all the experiments, we observed the wedge accretion according to a general piggy-back nucleation and propagation of thrusts. At the same time, the kinematic scenario interchanged between diachronous and synchronous activity of the major thrust fronts (Figs. 2c, 2d, 3c, 3d, 4c and 4d).

Two main factors control thrusts development: i) the occurrence of the two sedimentary tapers that vary their thickness and their mechanical behaviour normal to the direction of shortening, and ii) the occurrence of a total sand pack having a quite constant thickness (Fig. 1). The main result that we observed is that thickness variation triggers the non-cylindrical growth of thrust wedges, as already described in other sand box models, but, at the same time, diachronous propagation occurs in the opposite direction with respect to the single tapering models (Storti *et al.*, 2001; Soto *et al.*, 2003). Thrusts emerge systematically first in the thicker part of the sand pack and propagate laterally, reducing progressively their offset following the thickness reduction of the onlapping multilayer or of the depositional slope. In some cases, thrusts do not reach the other side of the apparatus (Figs. 2c, 3c and 4c). This first propagation often evolves in a linkage between the two diachronous thrust fronts; a single structure develops and remains active during the nucleation of a new asymmetric thrust front in its footwall (e.g. T4 and T5 in E2 experiment, figures 3c and 3d). When this happens, the curvature of the thrust traces generated on the two sides of the apparatus tends to be rectified in the central part of the model. Despite of this, the final geometry still shows a curved thrust front, where the central part is always retreated with respect to the lateral ones. This is well illustrated in the variation of  $L_p$

during deformation: along the three sections for each experiments,  $L_p$  (c) reaches always the minor length, whereas  $L_p$  (a) and  $L_p$  (b) alternate their length as a function of diachronic nucleation of thrusts (Figs. 2c, 3c and 4c).

According to the relationship proposed by Boyer (1995), the total thickness of each model (about 4 cm) and the high frictional values of basal detachment, the wedge accretes developing a small number of thrusts (only 3 in E1 and E3 models, 8 in E2). The internal variation of mechanical behaviour imposed to the models, on the other side, controls their structural style. In fact, we observe both a variation of the number of thrust and of the structural style moving from one side to the other of each model. In E2 model, in the multilayer eight thrusts front develop that progressively reduce to three on the depositional slope side. In this case, the accommodation of the along strike structural shortening occurs through the development of transfer zones, oblique ramps, and out of sequence thrusts.

In model E3, the occurrence of a weaker layer into the onlapping multilayer sequence triggers the development of back-thrust structures that varies laterally following the stratigraphic configuration.

In our experiments, the expected fast nucleation of new thrusts in the thinner part of the two overlying sand packs is completely deactivated, and their occurrence is highlighted in the difference of structural style and in a localization of strain. In fact, the central part of the model always retreats with respect to the other two sides, being a place of strong shortening and long life thrusts (e.g. T4/5 in E2 model, figure 3d).

The two thicker parts of the section controls mode of accretion and thrusts development, but this seems to occur independently from one side to the other of the models. Therefore, we assist to two sand packs, more or less coupled one to the other that developed together, but following different times. They are forced to proceed together in the second stage of individual thrust propagation, when the process of linkage occurred in the central part of the model. Here, in place of the hypothesized higher frequency of thrusting that should due to the occurrence of the two thinner zones, we observed a linkage process and synchronous thrusting, as required to account for the ongoing contraction (Figs. 2c, 2d, 3c, 3d, 4c and 4d).

## Conclusion

Complex geometries both in the pre-orogenic stratigraphy and in the upper crust are largely viewed as a control factor on the geometric organization of orogenic wedges. The occurrence of salients and regressions in thrust belt, as well as the number of thrust are generally linked to thickness variations of sedimentary sequences in most of the fold-and thrust belt all over the world (Boyer, 1995; Marshak and Wilkerson, 1992, Soto *et al.*, 2003, among many others).

We focused our analysis on the onlapping geometries, using laboratory sandbox experiments. Our attention was focalized on how this common sedimentary configuration could influence thrusts geometry and mode of accretion. In a simply geometrical analysis, our results show that onlapping geometries can cause asymmetric thrusts. The central part of our models (corresponding to the overlapping of the two thinner sequences) works as a transfer zone where deformation is more localized; here the thrust front is always retreated and out-of-sequence and long life thrusts

occur. Because of these geometrical differences, the kinematics of a growing orogenic wedge is deeply influenced. We observe, in fact, diachronous thrusting along strike, reactivation and under-thrusting alternating with simple piggy-back sequence. Our modeling results can be compared with natural examples from the Apennines, the southern Pyrenees, the Pindos (Greece) and the West Spitsbergen (Greenland) fold and thrust belts, among many others, where strain localization and diachronic thrusting affect thrust propagation in correspondence to complex stratigraphy (Speed *et al.*, 1984; Saalman and Thiedig, 2001; Storti *et al.*, 2001; Mazzoli *et al.*, 2002; Soto *et al.*, 2003; Skourlis and Doutsos, 2003).

## Acknowledgements

Experiments were performed at the Laboratorio di Modellazione Analogica, Università Roma Tre. We are grateful to Fabrizio Storti, Claudio Faccenna, Francesca Funicello, Valerio Acocella and Eugenio Carminati for useful discussions. This work was supported by project ex 60% (2006), University of Roma "La Sapienza", resp. Sabina Bigi.

## References

- BIGI, G., COSENTINO, D., PAROTTO, M., SARTORI, R. and SCANDONE, P. (1992): *Structural model of Italy, scale 1:500 000, 8 sheets*. C.N.R., P.F., Geodinamica.
- BIGI, S., CANTALAMESSA, G., CENTAMORE, E., DIDASKALOU, P., MICARELLI, A., NISIO, S., PENNESI, T. and POTETTI, M. (1997): The periadriatic basin (Marche-Abruzzi sector, Central Italy) during the Plio-Pleistocene. *Giorn. Geol.*, 59: 245-259.
- BOYER, S. E. (1995): Sedimentary basin taper as a factor controlling the geometry and advance of thrust belts. *Am. J. Sci.*, 295: 1220-1254.
- BUTLER, R. W. H. (1989): The influence of pre-existing basin structure on thrust system evolution in the western Alps. In: M. A. COOPER and G. D. WILLIAMS (eds): *Inversion tectonics*. *Geol. Soc. Spec. Publ.*, 44: 105-122, London.
- CARMINATI, E. and SANTANTONIO, M. (2005): Control of differential compaction on the geometry of sediments onlapping paleoescarpments: Insights from field geology (Central Apennines, Italy) and numerical modeling. *Geology*, 33: 353-356.
- DOGLIONI C., MONGELLI F. and PIERI P. (1994): The Puglia uplift (SE-Italy): an anomaly in the foreland of the Apenninic subduction due to buckling of a thick continental lithosphere. *Tectonics*, 13, 5: 1309-1321.
- GILLCRIST, R., COWARD, M. P. and MUGNIER, J. L. (1987): Structural inversion and its control: examples from the alpine foreland and the French Alps. *Geodin. Acta*, 1: 5-34.
- LIU, H., MCCLAY, K. R. and POWELL, D. (1992): Physical models of thrust wedges. In: K. R. MCCLAY (ed): *Thrust tectonics*, Chapman & Hall, London: 71-81
- MALAVIEILLE, J. (1984): Modelisation experimentale des chevauchements imbriques: application aux chaines de montagnes. *B. Soc. Géol. Fr.*, 26: 129-138.
- MARSHAK, S. and WILKERSON, M. S. (1992): Effect of overburden thickness on thrust belt geometry and development. *Tectonics*, 11, 3: 560-566.
- MAZZOLI, S., DEIANA, G., GALDENZI, S. and CELLO, G. (2002): Miocene fault-controlled sedimentation and thrust propagation in the previously faulted external zones of the Umbria-Marche Apennines, Italy. *Stephan Mueller Spec. Publ. Series*, 1: 195-209.
- MCCLAY, K. R. (1990): Extensional fault systems in sedimentary basins: a review of analogue model studies. *Mar. Petrol. Geol.*, 7: 206-233.
- MULUGETA, G. (1988): Modelling the geometry of coulomb thrust wedges. *J. Struct. Geol.*, 10: 847-859.
- ORI, G. G., SERAFINI, G., VISENTIN, C., RICCI LUCCHI, F., CASNEDI, R., COLALONGO, M. L. and MOSNA, S. (1991): The Pliocene-Pleistocene Adriatic foredeep (Marche and Abruzzo, Italy). An integrated approach to surface and subsurface geology. In: 3<sup>rd</sup> E. A. P. G., *Conference, Florence, Italy, Adriatic Foredeep Field Trip Guide Book*, 70 pp.
- ROSSI, D. and STORTI, F. (2003): New artificial materials for analogue laboratory experiments: aluminium and siliceous microspheres. *J. Struct. Geol.*, 25: 1893-1899.

- SAALMAN, K. and THIEDIG, F. (2001): Tertiary West Spitsbergen fold and thrust belt on Broggerhalvoya, Svalbard: Structural evolution and kinematics. *Tectonics*, 20, 6: 976-998.
- SKOURLIS, K. and DOUTSOS T. (2003): The Pindos Fold-and-thrust-belt (Greece): inversion kinematics of a passive continental margin. *Int. J. Earth Sci.*, 92: 891-903.
- SOTO, R., STORTI, F., CASAS, A. M. and FACCENNA, C. (2003): Influence of along-strike pre-orogenic sedimentary tapering on the internal architecture of experimental thrust wedges. *Geol. Mag.*, 140, 3: 253-264.
- SPEED, R., WESTBROOK, G., MASCLE, A., BIJU-DUVAL, B., LADD, J., SAUNDERS, J., STEIN, S., SCHOONMAKER, J. and MOORE, J. (eds) (1984): *Lesser Antilles Arc and adjacent terranes, Ocean Margin Drilling Program, Regional Atlas Series, Atlas 10, 27 sheets*. Marine Science International, Woods Hole, Massachusetts.
- STORTI, F. (1997): Simulazione di anticlinali di rampa e cunei di accrezione mediante modellizzazione analogica. *B. Soc. Geol. Ita.*, 116: 17-38.
- STORTI, F., SALVINI, F. and MCCLAY, K. (2000): Synchronous and velocity-partitioned thrusting, and thrust polarity reversal in experimentally produced, doubly-vergent thrust wedges: implications for natural orogens. *Tectonics*, 19: 378-396.
- STORTI, F., SOTO, R., FACCENNA, C. and CASAS-SAINZ, A. (2001): Role of the backstop-to-cover thickness ratio on vergence partitioning in experimental thrust wedges. *Terra Nova*, 13: 413-417.
- THOMAS, W. A. (1990): Controls on locations of transverse zones in thrust belts. *Eclogae Geol. Helv.*, 83: 727-744.